



7th International Conference on Fatigue Design, Fatigue Design 2017, 29-30 November 2017,
Senlis, France

A numerical method for determining the fatigue strength of welded joints with a significant improvement in accuracy

Lener, G.^a; Lang, R.^a; Ladinek, M.^a; Timmers, R.^a

^a*Department of Engineering Sciences, Unit of Steel Construction and Mixed Building Technology,
University of Innsbruck, 6020 Innsbruck, Austria*

Abstract

Modelling fatigue assessments for welded components is a challenging task as to achieving accurate results. Several influence factors reduce accuracy and often the difference between the calculated and the effective fatigue life is located in the range of factor 10 and above. This conference paper presents two advanced methods which allow the achievement of better accuracy. The main aspect consists in taking the geometry into account, a procedure that leads, though, to the need of adapting the existing methods for fatigue assessment. One of these advanced methods is used to examine a detail which has been welded with different welding processes and on different positions.

© 2018 The Authors. Published by Elsevier Ltd.
Peer-review under responsibility of the scientific committee of the 7th International Conference on Fatigue Design.

Keywords: fatigue assesment; laser scan; real geometry; welded components

1. Introduction

In steel and mechanical engineering, there are numerous concepts dealing with the calculation of fatigue strength in the range of high cycle fatigue of mild-steel welded structures. However, in many cases and due to various reasons, the accuracy in the computational determination of the fatigue strength and of the possible number of stress cycles leading to failure is very imprecise. Assessment procedures applied in practical engineering are sometimes built on more or less pure empiric findings rather than on the numerical description of the failure process. Fatigue assessment is often performed by post-processing elastic stress fields, neglecting the local yielding which often occurs in notched areas. From a theoretical point of view, the reason for such a procedure may be the common understanding of the fatigue problem as being of brittle nature, at least on the scale of engineering consideration. In addition, certain aspects of cyclic plasticity, which are not fully understood, do not have to be dealt with. From a

practical point of view, elasto-plastic finite element calculations, which are said to be time consuming are avoided [1].

It is well known, that under the assumption of linear-elastic material behavior, stresses are high in notched areas; therefore, a direct comparison to the materials fatigue strength cannot be performed. Besides the nominal stress approach, many of the design concepts apply a form of effective stress or strain definition based on various underlying ideas.

Another issue is the inaccurate consideration of the weld geometry in assessment approaches considering welded components. The weld geometry is an important factor as additional stress concentrations can be introduced by each individual weld form. Consequently, if an increase in accuracy is desired, an evaluation of the actual geometry of the welded components including the welded connection is unavoidable. This can be realized through the consideration of the real weld surface, which can be obtained by 3D laser scanning. Such procedures have been applied in recent research [2,3]. Even though the direct incorporation of data obtained by laser scanning for industry application seems difficult on first sight, the application in the framework of quality control or for the prediction of fatigue life of highly stressed components is thinkable [4]. Anyway, the implementation of the real weld geometry in the assessment approach seems promising in order to capture the real emerging notch stresses.

Using the actual geometry for fatigue assessment leads to the challenge of including notch sensitivity in the computation procedure. In the contribution at hand, we present an approach based on the consideration of the real weld geometry. Through the application of Weibull statistics, the effect of the highly stressed volume can be captured and promising results in terms of accuracy in the prediction of fatigue life can be reported.

The contribution is structured as follows. In section 2.1 popular support approaches are shortly discussed. After that, the application of an implicit gradient approach is introduced in order to serve as tool to obtain an effective stress definition. Section 2.3 discusses the basics of the Weibull statistics and the following one, the combination of both concepts. After the numerical procedure is shown in section 3, the approach for the laser scanning of the weld geometry is explained and the application of the probabilistic approach to estimate the fatigue life of welded components is demonstrated.

Nomenclature

$\Delta\sigma$	stress range
$\Delta\sigma_n$	nominal stress range
$\Delta\sigma_{CR}$	reference value of characteristic stress range at 2 Mio. cycles
σ_D	stress at fatigue limit
σ_{eff}	effective stress
σ_k	notch stress
$\sigma_{k\max}$	maximum notch stress
ξ^*	shape factor of Weibull distribution
η_k	notch sensitivity
μ	part of threshold in life time
ν	Poisson's ratio
ν^*	stress modifactor (Volume method)
ρ	intrinsic length (Neuber method)
Ψ	scaling factor
A	area
A_0	reference value of stressed area
B, C	constants (Volume method)
E	Young's modulus
EV	expected value

G	weighting function
M_i, N_i	bending moment, axial forces
N	cycles
N^{cal}	calculated cycles
N_C	characteristic cycles
N_{test}	tested cycles until crack initiation
P_f	probability of failure
P_s	probability of survival
\bar{W}	section modulus
a_*	constant factor
a	intrinsic length (Peterson method)
b_*	defect of size b
b	intrinsic length (Sheppard method)
b_c	characteristic size
C	rate of variance
m	slope of S-N-curve
n	function to consider stress gradient
\bar{n}	normal vector to the surface
p	constant factor
q	quantile distance
r	correlation coefficient
s	factor to consider type of stress/strain state (Neuber method)

2. Approaches of fatigue assessment based on notch stresses

2.1. General overview

The main complication with fatigue assessment consists in the fact that not the maximal notch stress determines fatigue life but rather some sort of reduced stress. The reduction of this stress depends on the sharpness of the notch, the specific material and the approach used. The elastic stress field around the notch is further processed for the fatigue assessment by applying various concepts for stress reduction (termed ‘support approaches’ in the following). Self-evidently, this is only necessary when local yielding is not considered through plasticity. From an historical point of view, it shall be mentioned that the combination of the elastic stress field and the use of a support approach has a long tradition and it is applied in the most popular assessment approaches. For the sake of completeness, it shall also be mentioned/specified that local yielding can be considered in the strain-life approach (ϵ -N) to fatigue, an aspect which is not discussed in this contribution. Fig. 1 shows some common approaches used to calculate effective stresses in notches.

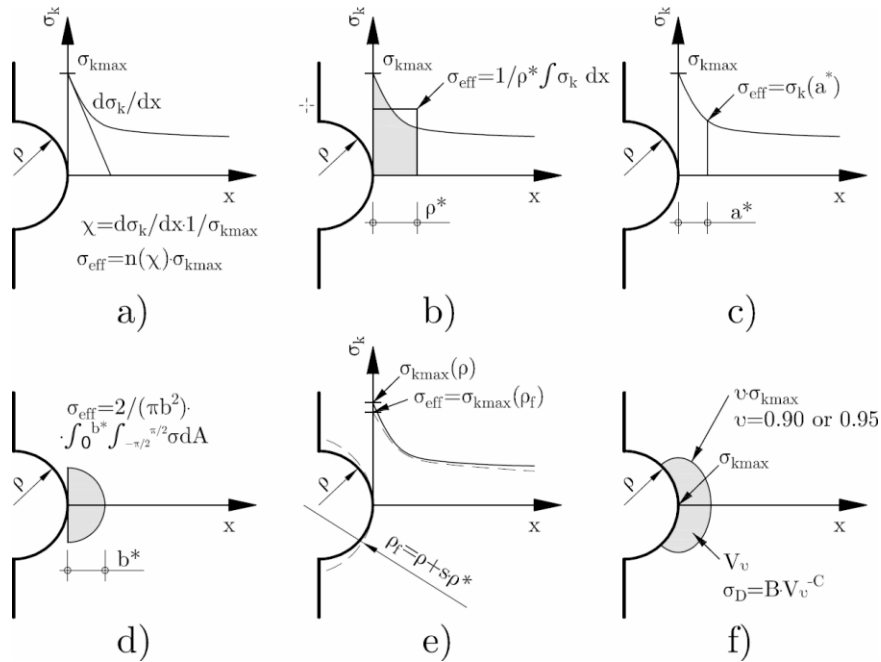


Fig. 1. a) Siebel/Stieler [5] b) Neuber [6] c) Peterson [7] d) Sheppard [8] e) Neuber/Radaj [6,9] f) Kuguel/Sonsino [10,11]

The explanation of this effect illustrated above was described by several researchers in the past. Neuber [6] called this effect “micro support”, Taylor [12] unified some of these approaches into the “Theory of critical distances” (TCD). Equation (1) and Fig. 1a-e show these deterministic approaches.

$$(1)$$

$$\sigma_{eff} = \eta_k^* \sigma_k$$

Equation (1) omits one important influence effect: the statistical size effect which is shown in Fig. 1f. Zhang [13] and Yao [14] separated the influence factors of notch stress effects into these two types: an effect of stress field and an effect of the size of high stressed surface and of high stressed volume.

What seems easy to divide at first can be highly complicated, though. Fig. 2 shows some problems deriving from notch stress fatigue: Fig. 2a/b displays the effects of a stress field but can also be interpreted as some sort of size effect; in contrast Fig. 2c is obviously a statistical size effect.

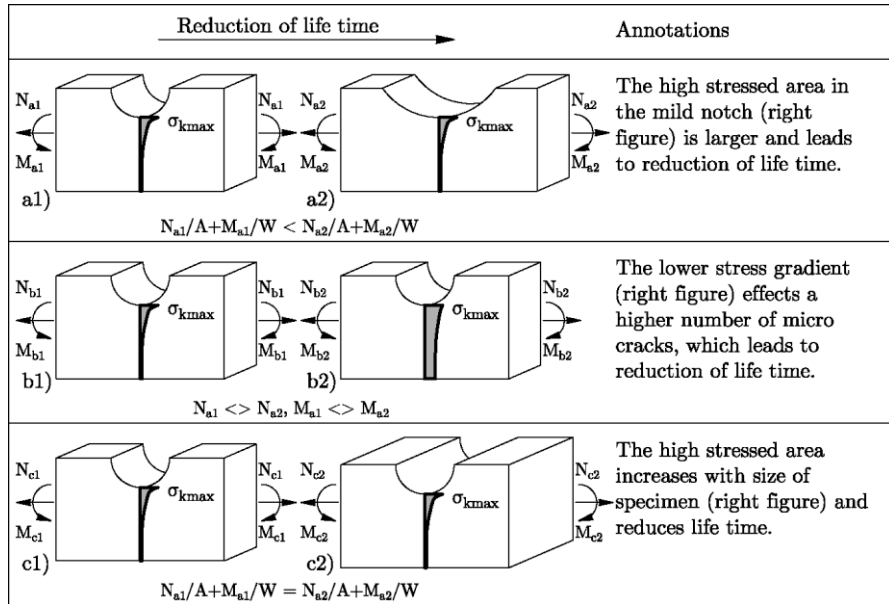


Fig. 2. Problems of notch fatigue [2]

In order to take the real notch geometry of a welded component into account, both methods must be adopted. Chapter 2.2 shows a variant of a deterministic support theory; in chapter 2.3 a probabilistic model is explained in order to cover the statistical size effect.

2.2. Implicit gradient model

The application of a non-local theory in fatigue design has been recently introduced [15]. The main idea, similar to the support approach concept, consists in assuming that not the highest but rather over a certain volume averaged stress or strain is critical for fatigue crack initiation. In some cases, this is argued by taking into consideration the general non-local characteristics of the damage process [13] or by addressing the influence of the materials microstructure [16,17]. From a theoretical point of view, Zhang [13] developed the direct relation between non-local theory and popular support approach concepts by showing that some of these concepts consist in special cases of the non-local approach. A general framework can be formulated by utilizing the elastic stress field σ_k and an integral kernel G [13]. This general relation is also used by others e.g. [18] and it is addressed by Equation (2) and Fig. 3.

$$\sigma_{eff}(\vec{x}) = \frac{1}{\Psi(\vec{x})} \int_V G(\vec{x}, \vec{x}') \sigma_k(\vec{x}') dV_{x'} \tag{2}$$

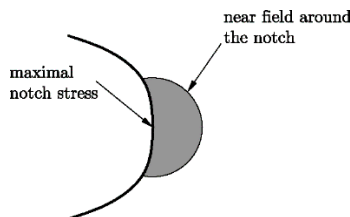


Fig. 3. Near field around the notch [15]

\underline{G} represents a weighting function, Ψ a scaling function, V the volume around the notch, \bar{x} the point of interest and x the far point. The modification of the weight function G is a matter of recent discussions and reference and the interested reader is referenced to the literature and the references therein [19].

The commonly applied form of the non-local framework is the integral averaging approach (see Equation (2)). There are different alternatives of the weighting function; the application of the Gauss function seems to be the most popular one, though. By using this procedure, the integral averaging approach can be transferred to an implicit gradient formulation as shown by Peerlings [2,15,18,20,21]. The implicit formulation is shown in Equation 3 and can easily be solved numerically.

$$\sigma_{eff}(\bar{x}) - a\nabla^2\sigma_{eff}(\bar{x}) = \sigma_k(\bar{x}) \quad (3)$$

On free surfaces, appropriate Neumann boundary conditions must be included (Equation (4)).

$$\frac{\partial\sigma_{eff}(n)}{\partial\vec{n}} = 0 \quad (4)$$

By applying a support concept in the form of Equation (3), an additional parameter is introduced. The parameter \mathbf{a} governs the volume, which contributes to the averaging procedure. The determination of the correct size of this parameter is not straightforward and, hence, various approaches come to hand. As stated before, it is often argued that this parameter has to be linked to the materials micro-structure; thus, making the approach micro-structure sensitive seems to be a promising idea. Other researchers suggest inverse analysis or procedures fitted to measured strain profiles. A comprehensive discussion on this issue is presented in [22]. A practical approach for the determination of the size of this parameter from TCD has also been suggested [16,23].

For the contribution at hand, the size of the parameter \mathbf{a} was determined from parametric finite element studies via procedure of optimization.

2.3. Probabilistic approach – Weibull model

A Weibull based probabilistic model can be used in order to cover the statistical size effect. The model assumes the probability to discover a defect of size b in an area or volume. b_c is the characteristic size and \mathcal{C} is a rate of variance. The probability of discovering a defect less than b is shown in Equation (5).

$$P_b = \exp\left(-\left(\frac{b}{b_c}\right)^{\mathcal{C}}\right) \quad (5)$$

If this model is transferred to treat fatigue problems see Equation (6).

$$P_s(\Delta\sigma) = \exp\left(-\left(\frac{\Delta\sigma}{\Delta\sigma_C}\right)^\kappa\right) \quad (6)$$

The probability of failure leads to Equation (7) when several volumes or areas are loaded with different stress levels.

$$P_f = 1 - \prod_{i=1}^n P_s(\Delta\sigma) \quad (7)$$

When considering only surfaces with possible different sizes, the equation can be rearranged to Equation (8), where the parameter ζ is the shape factor of the Weibull distribution. The meaning of A_i can be seen in Fig. 5 on a FEM-mesh.

$$P_f(\Delta\sigma, N) = 1 - \prod_{i=1}^n \exp\left(-\frac{A_i}{A_0} \left(\frac{\log_{10} N}{\log_{10} N_{C,i}}\right)^{\zeta_i}\right) \quad (8)$$

with

$$\zeta_i = p \cdot \log_{10} N_{C,i} \quad (9)$$

and using a linear S-N-curve (Equation (10))

$$\log N_{C,i} = \log 2 \cdot 10^6 - m(\log \Delta\sigma_i - \log \Delta\sigma_{CR}) \quad (10)$$

2.4. Combination of both approaches

Both models can be used solely or in combination according to Equation (1). The calculation sequence is shown in chapter 3. The Weibull model can be adapted for notch stresses σ_k (without using the Implicit Gradient Model) or for the effective stresses σ_{eff} according to Equation (2).

3. Calculation sequence when using the Finite Element Method

3.1. Flow diagram

The following Fig. 4 shows the calculation steps required when using the briefed methods.

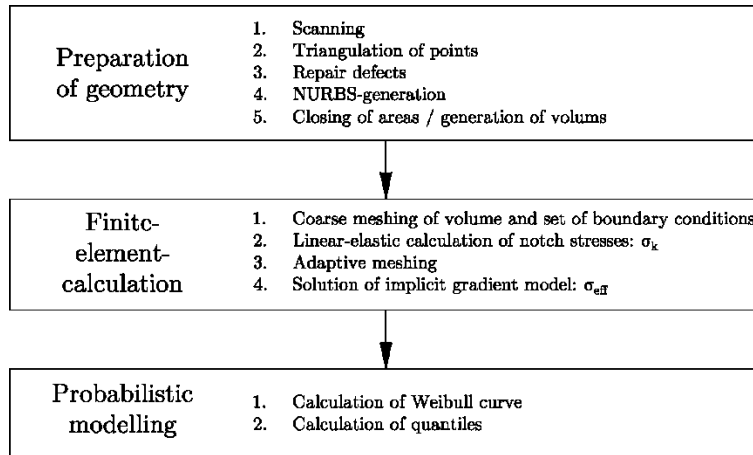


Fig. 4. Calculation sequence [24]

In order to evaluate Equation (8), it is necessary to calculate the area of influence corresponding to the nodes. Fig. 5 shows this task. It must be pointed out that this task can be calculated in several different ways, including the use of energy approaches or like a roof design.

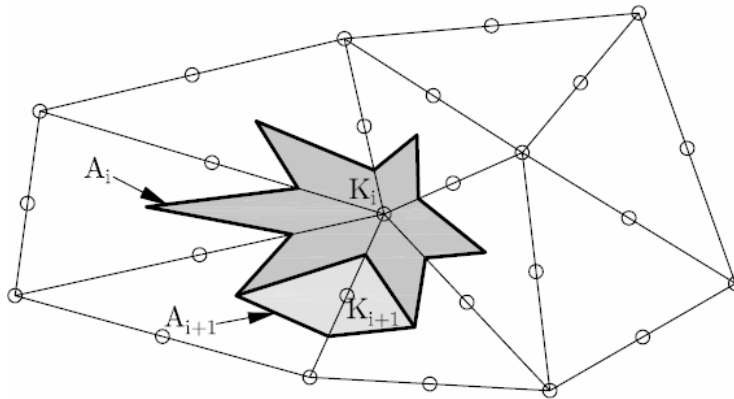


Fig. 5. Areas of influence and nodes on Finite Element Calculations [24]

3.2. Scan technics

It is necessary to scan the details which have to be evaluated. This work can be done with today's laser scanning systems. A FARO mobile laser scan system was used for the work described in this paper. The resolution of the scan system is 0.05mm and the accuracy within 0.035mm. The statistical significance is twice the standard deviation. The so captured points were triangulated into a mesh and further into a C1-continuous NURBS surface. The C1 continuity avoids numerical singularities when calculating with FEM.

4. Application of a probabilistic approach on welded specimens

4.1. Input parameters and design of specimens

In this chapter the methods presented in chapter 2.3, according to the calculation sequence shown in chapter 3, are used to classify welded details as shown in Fig. 6, 7 and 8. The weld detail consists of a plate with a stiffener with fillet welds. The fatigue cracks would occur on the surface and the detail is classified as T-detail with FAT80 according to existing standards [25].

The weld details were produced by using different welding procedures and by different positions (Table 1). Welding procedure 111 consists of manual metal arc welding (MMA) and procedure 135 is metal-arc active gas welding (MAG) according to [26].

Table 1. Details: Welding procedures and welding positions.

Detail	Welding procedure	Welding position
PA-111	111 (MMA)	PA (flat position)
PA-135	135 (MAG)	PA (flat position)
PB-111	111 (MMA)	PB (horizontal vertical position)
PB-135	135 (MAG)	PB (horizontal vertical position)
PE-111	111 (MMA)	PE (overhead position)
PE-135	135 (MAG)	PE (overhead position)
PF-111	111 (MMA)	PF (vertical up position)
PF-135	135 (MAG)	PF (vertical up position)
PG-111	111 (MMA)	PG (vertical down position)
PG-135	135 (MAG)	PG (vertical down position)

The weld details are calculated by applying the Finite Element Method using linear elastic material models with the following material values:

$$E = 210000\text{N/mm}^2 \quad (11)$$

$$\nu = 0.3$$

Input parameters from [2], shown in Fig. 6:

$$A_0 = 1\text{mm}^2$$

$$m = 2.85 \quad (12)$$

$$\Delta\sigma_{CR} = 357.7\text{N/mm}^2$$

$$p = 7.85$$

As loading parameter it is used a nominal stress range according to Equation (13).

$$\Delta\sigma_n = 120\text{N/mm}^2 \quad (13)$$

This stress range was chosen because it would lead to results in the area of high cycle fatigue.

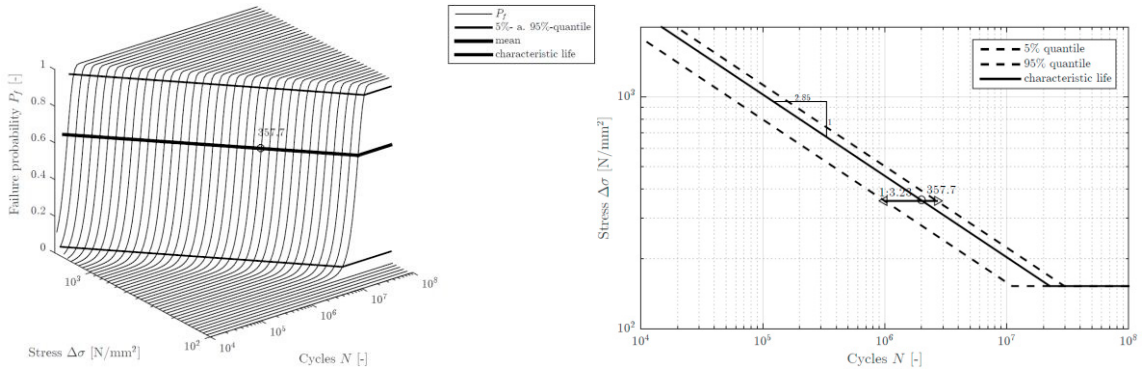


Fig. 6. Used Parameters of Equation (12)

A 50mm width part was cut out from the welded details and classified (Fig. 7).

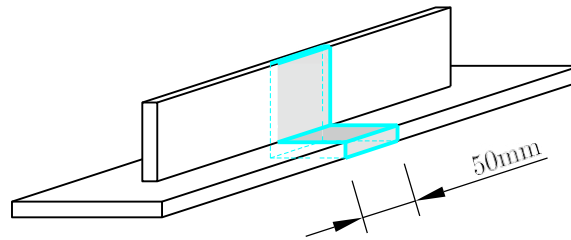


Fig. 7. Specimens [4]

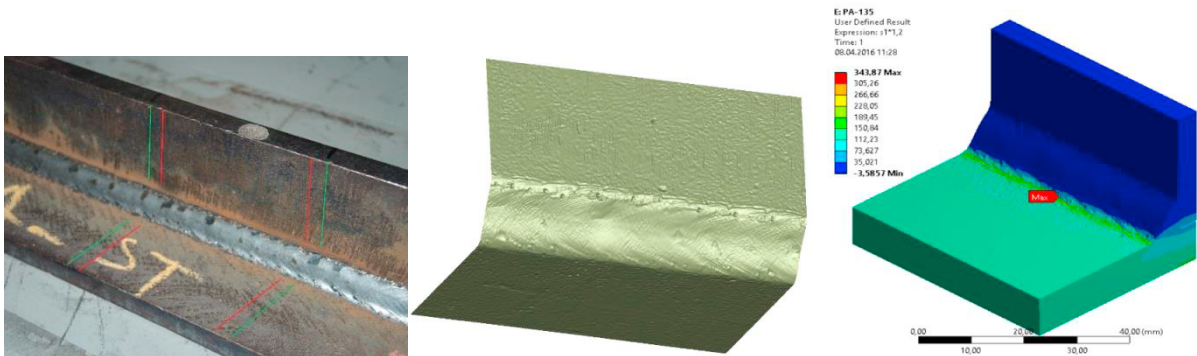


Fig. 8. a) PA135 specimen b) PA135 NURBS c) PA135 stresses [27]

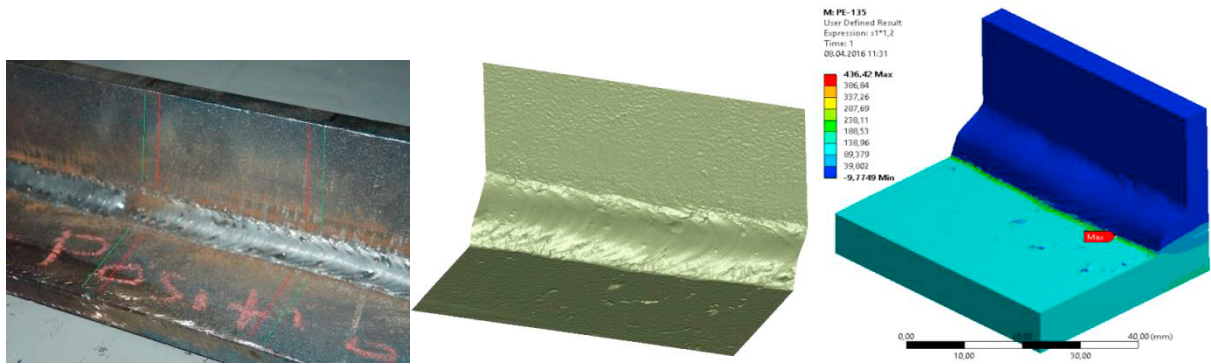
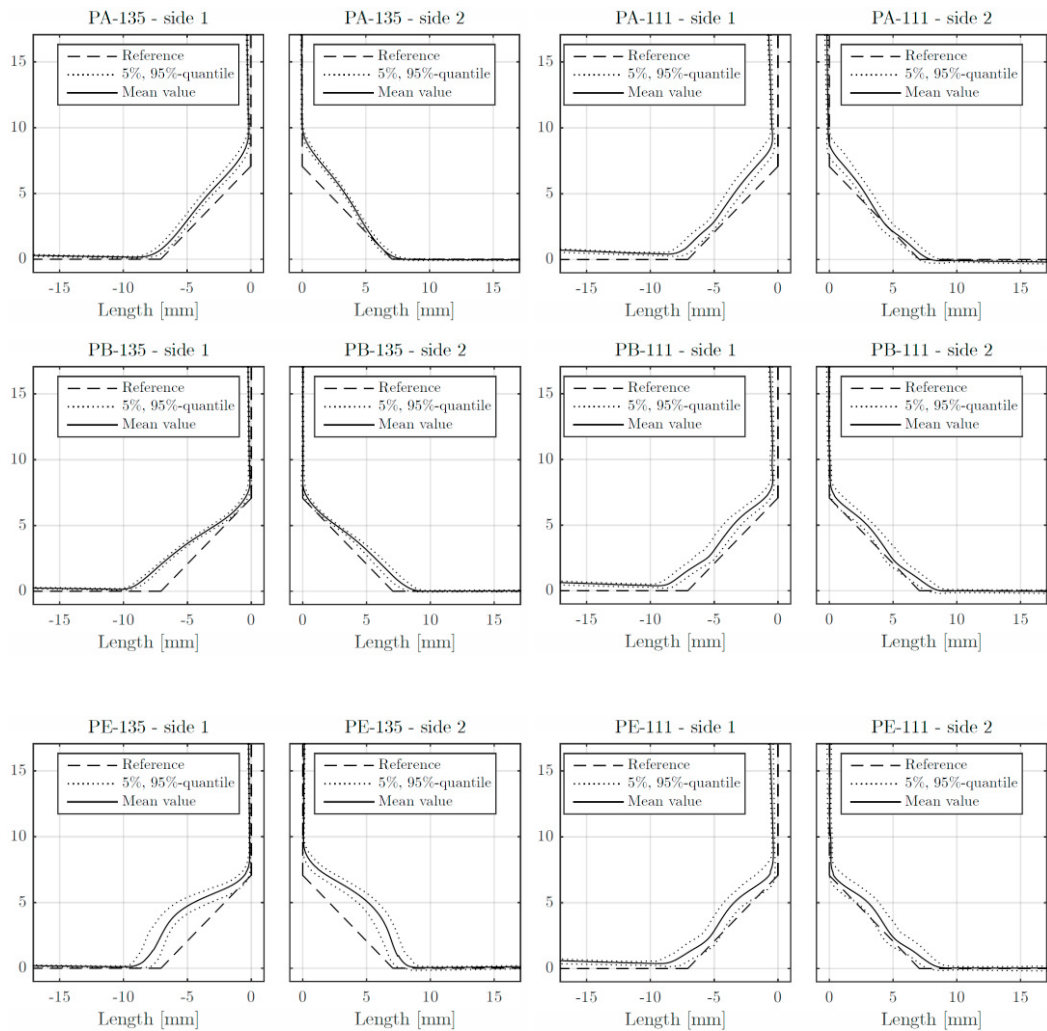


Fig. 9. a) PE135 specimen b) PE135 NURBS c) PE135 stresses [27]



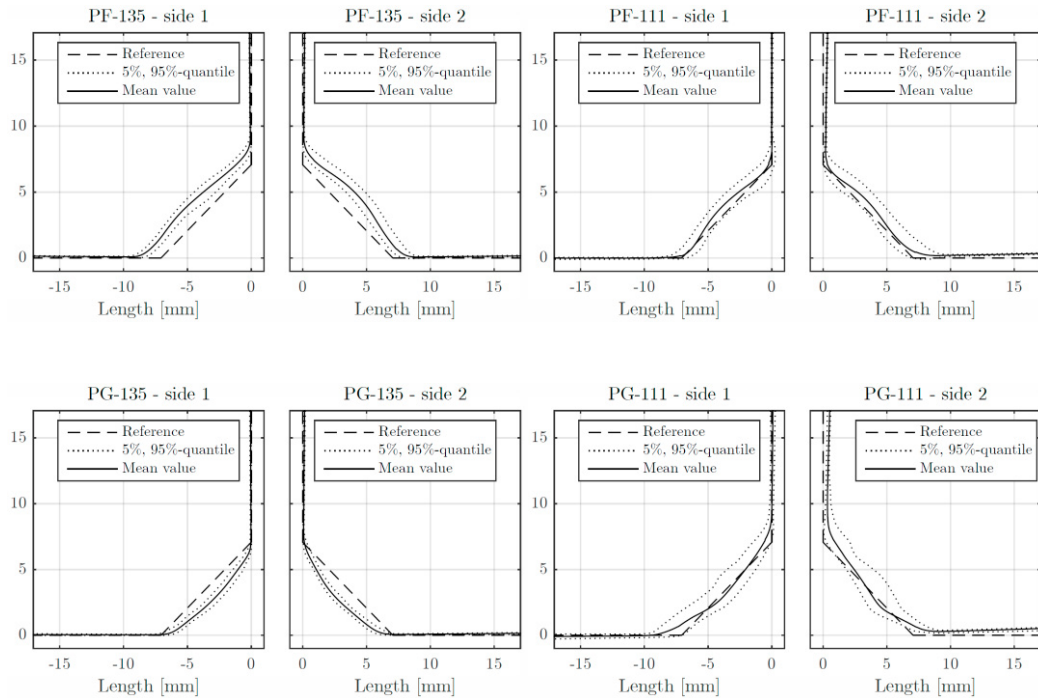


Fig. 10. Deviations of the scanned geometry from the reference geometry [4]

4.2. Results

The results of the calculation are shown in Fig. 11 and 12. Fig. 11 shows the stress histogram of the welded details for a nominal stress range of $\Delta\sigma_n = 120\text{N/mm}^2$. Fig. 12 shows the failure curves calculated according to Equation (8). As expected, the procedure PE-135 is very bad in terms of fatigue strength. Mild notched toes (PA-135, PB-135 and PG-135) show higher fatigue life spans. PF-135 presents locally sharp notches which determines fatigue life. The welding procedure 111 (MMA) shows generally reduced life spans. This results from sharper local notches and higher weld penetration. These effects affect especially the specimens PA-111 and PF-111. The higher fatigue strengths of PE-111 and PG-111 are due to the flat transition between base plate and stiffener.

Every analyzed weld detail would achieve with high probability the FAT80. Table 2 shows the probabilities of failure and the calculated life times.

Table 2. Calculated life time.

FAT / detail	N95	N50	N05	N05/N95
112	1.626.000	-	-	-
100	1.157.000	-	-	-
90	844.000	-	-	-
80	593.000	-	-	-
71	414.000	-	-	-
63	289.000	-	-	-

PA-111	752.000	1.533.000	2.324.000	3.09
PB-111	924.000	1.878.000	2.840.000	3.08
PE-111	1.122.000	2.284.000	3.459.000	3.08
PF-111	745.000	1.525.000	2.319.000	3.11
PG-111	1.190.000	2.434.000	3.694.000	3.10
PA-135	1.579.000	3.195.000	4.819.000	3.05
PB-135	1.376.000	2.790.000	4.212.000	3.06
PE-135	820.000	1.671.000	2.533.000	3.09
PF-135	1.145.000	2.311.000	3.480.000	3.04
PG-135	1.292.000	2.626.000	3.973.000	3.08

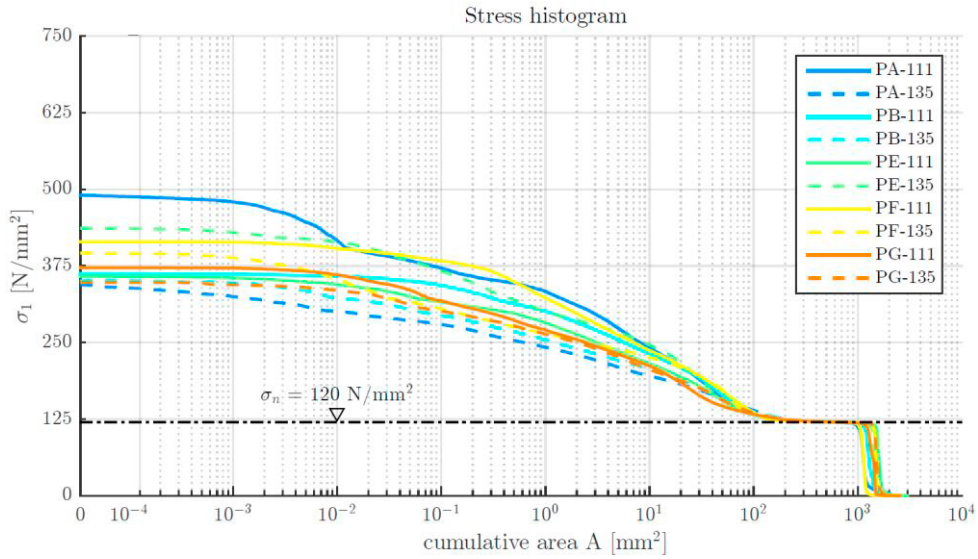


Fig. 11. Stress histogram [27]

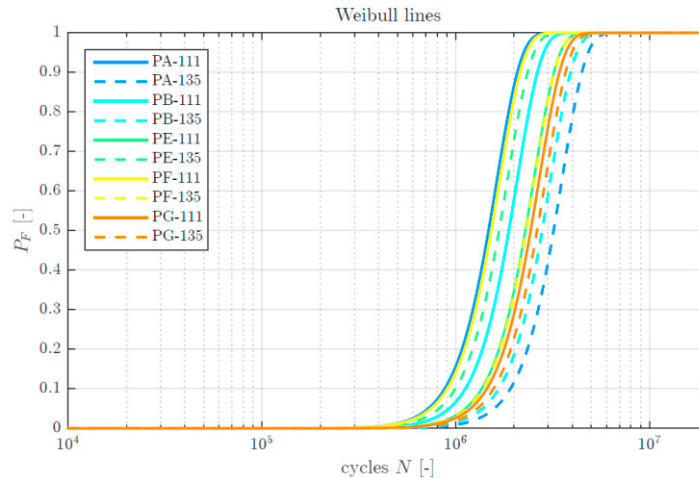


Fig. 12. Calculated Weibull curves [27]

It ought to be pointed out that the evaluation has some fuzziness. In fact, the procedure has some deviations and the choice of the cutting takes place subjectively. Taking into account the analyzed details, though, it can be asserted that there is no perfect weld position but some positions can provide better results with less effort.

5. Discussion of the approaches and results

The presented approach enables not only the fatigue assessment of welded joints, but it also allows individual features of the analyzed specimen to be considered in the assessment. Through the consideration of the real weld geometry, real notch stresses, resulting from various weld radii, can be used for the prediction of fatigue life as well as for the definition of the size of the highly stressed areas; an aspect that is well known as playing a role in influencing fatigue life. It seems self-evidently, at least to some degree, that the application of reality based weld geometries helps to increase the accuracy of predictions. Some assessment approaches regarding welded joints use either none, or simplified weld representations in FE calculations; procedures which raise the question whether a sufficient consideration, not only of the welded joints' stiffness, but also of the notch stresses occurs in reality. Taking into account the well-known fact that a small increase in stress may lead to a dramatic reduction of fatigue life, it seems crucial to consider the notch stresses as realistically as possible.

The probabilistic approach was applied on ten weld details made of the same material and layout but welded with different welding procedures and on different positions. The influence of these execution parameters on the fatigue life of the components can be shown in a clear way using the method discussed in this paper.

References

- [1] Susmel L. Modified Wöhler curve method, theory of critical distances and Eurocode 3: A novel engineering procedure to predict the lifetime of steel welded joints subjected to both uniaxial and multiaxial fatigue loading. *International Journal of Fatigue* 2008;30(5):888–907.
- [2] Lang R, Lener G. Application and comparison of deterministic and stochastic methods for the evaluation of welded components' fatigue lifetime based on real notch stresses. *International Journal of Fatigue* 2016;93:184–93.
- [3] Kaffenberger M. *Schwingfestigkeit von Schweißnahtenden und Übertragbarkeit von Schweißverbindungs-Wöhlerlinien*. Darmstadt, Darmstadt: Techn. Univ; 2012.

- [4] Lang R, Lener G, Schmid J, Ladinek M. Schweißnahtbewertung basierend auf 3D-Laserscanning: Praktische Anwendung eines mobilen Laserscansystems zur Oberflächenbewertung von Schweißnähten – Teil 1. *Stahlbau* 2016;85(5):336–43.
- [5] Stieler M. Untersuchungen über die Dauerschwingfestigkeit metallischer Bauteile bei Raumtemperatur. Stuttgart, T. H., F. f. Maschinenw., Diss. v. 26. Juni 1954. (Stuttgart); 1954.
- [6] Neuber H. Kerbspannungslehre: Theorie der Spannungskonzentration Genaue Berechnung der Festigkeit. 3rd ed. Berlin, New York: Springer-Verlag; 1985.
- [7] Peterson R. Notch-sensitivity. *Metal Fatigue* 1959:293–306.
- [8] Sheppard SD. Field Effects in Fatigue Crack Initiation: Long Life Fatigue Strength. *J. Mech. Des.* 1991;113(2):188.
- [9] Radaj D, Vormwald M. Ermüdungsfestigkeit: Grundlagen für Ingenieure. 3rd ed. Berlin: Springer; 2007.
- [10] Kuguel R. A relation between theoretical stress concentration factor and fatigue notch factor deduced from the concept of highly stressed volume. *Proc. ASTM* 1961;61:732–44.
- [11] Sonsino CM. Zur Bewertung des Schwingfestigkeitsverhaltens von Bauteilen mit Hilfe örtlicher Beanspruchungen: Evaluation of components' fatigue behaviour on the basis of local strains/stresses. *Konstruktion* 1993;45(1):25–33.
- [12] Taylor D. Geometrical effects in fatigue: a unifying theoretical model. *International Journal of Fatigue* 1999;21(5):413–20.
- [13] Zhang G. Method of effective stress for fatigue: Part I – A general theory. *International Journal of Fatigue* 2012;37:17–23.
- [14] Yao W. A verification of the assumption of anti-fatigue design. *International Journal of Fatigue* 2001;23(3):271–7.
- [15] Peerlings RHJ. Enhanced damage modelling for fracture and fatigue. Eindhoven: Technische Universiteit Eindhoven; 1999.
- [16] Askes H, Susmel L. Understanding cracked materials: Is Linear Elastic Fracture Mechanics obsolete? *Fatigue Fract Engng Mater Struct* 2015;38(2):154–60.
- [17] Peerlings RHJ, Brekelmans WAM, Borst R de, Geers MGD. Gradient-enhanced damage modelling of high-cycle fatigue. *Int. J. Numer. Meth. Engng.* 2000;49(12):1547–69.
- [18] Peerlings RHJ, Geers MGD, Borst R de, Brekelmans W. A critical comparison of nonlocal and gradient-enhanced softening continua. *International Journal of Solids and Structures* 2001;38(44-45):7723–46.
- [19] Simone A, Askes H, Sluys LJ. Incorrect initiation and propagation of failure in non-local and gradient-enhanced media. *International Journal of Solids and Structures* 2004;41(2):351–63.
- [20] Tovo R, Livieri P. An implicit gradient application to fatigue of sharp notches and weldments. *Engineering Fracture Mechanics* 2007;74(4):515–26.
- [21] Maggiolini E, Livieri P, Tovo R. Implicit gradient and integral average effective stresses: relationships and numerical approximations. *Fatigue Fract Engng Mater Struct* 2014:n/a.
- [22] Bažant ZP, Jirásek M. Nonlocal Integral Formulations of Plasticity and Damage: Survey of Progress. *J. Eng. Mech.* 2002;128(11):1119–49.
- [23] Susmel L, Askes H, Bennett T, Taylor D. Theory of Critical Distances versus Gradient Mechanics in modelling the transition from the short to long crack regime at the fatigue limit. *Fatigue Fract Engng Mater Struct* 2013;36(9):861–9.
- [24] Lang R. Ein Beitrag zur Bestimmung der Anrisslebensdauer geschweißter Bauteile [Dissertation]. Innsbruck: Universität Innsbruck; 2015.
- [25] Österreichisches Normungsinstitut. ÖNORM EN 1993-1-9: Eurocode 3: Bemessung und Konstruktion von Stahlbauten Teil 1-9: Ermüdung; 2005.
- [26] Österreichisches Normungsinstitut. ÖNORM EN ISO 4063: Schweißen und verwandte Prozesse - Liste der Prozesse und Ordnungsnummern; 2011.
- [27] Lang R, Lener G. Schweißnahtbewertung basierend auf 3D-Laserscanning: Praktische Anwendung eines mobilen Laserscansystems zur Oberflächenbewertung von Schweißnähten – Teil 2. *Stahlbau* 2016;85(6):395–408.